ANTICANCER RESEARCH *41*: 4837-4855 (2021)
doi:10.21873/anticanres.15298

REIC/Dkk-3 Gene Therapy Induces Immunogenic Cell Death in a Mouse Model of Malignant Mesothelioma

KENJI ARAKI[1,2], NAOYA YAMAMURO[2], NAHOKO TOMONOBU[3] and HIROMI KUMON[1,4]

[1]*Innovation Center Okayama for Nanobio-targeted Therapy, Okayama University, Okayama, Japan;*
[2]*Watarase Research Center, Kyorin Pharmaceutical Co., Ltd., Nogi-machi, Japan;*
[3]*Department of Cell Biology, Okayama University Graduate School of Medicine, Dentistry and Pharmaceutical Sciences, Okayama, Japan;*
[4]*Niimi University, Niimi, Japan*

Abstract. *Background/Aim: The adenovirus vector–carrying reduced expression in immortalized cell (REIC) gene (Ad-REIC) increases endoplasmic reticulum stress chaperone GRP78/BiP expression and induces the JNK-mediated apoptotic pathway. We aimed to determine whether Ad-REIC–induced apoptotic cell death can trigger immunogenic cell death (ICD). Materials and Methods: We examined the emission of damage-associated molecular patterns in vitro and the vaccination effect in vivo. We determined the immunological changes in the tumour microenvironment by putative ICD inducers and the combined effects of immune checkpoint blockade therapies. Results: Ad-REIC induced the release of high-mobility group box 1 and adenosine triphosphate and the translocation of calreticulin in murine mesothelioma AB12 cells. The vaccination effect was elicited by Ad-REIC treatment in vivo. The effect of Ad-REIC was potentiated by anti-cytotoxic T-lymphocyte–associated protein 4 antibody treatment in a murine mesothelioma AB1-HA cell model. Conclusion: Ad-REIC induces ICD in malignant mesothelioma.*

The reduced expression in immortalized cell (*REIC*) gene was first identified at the Okayama University (Okayama, Japan), and was described as a gene whose expression is down-regulated in immortalized human fibroblasts OUMS-24 (1). The *REIC* gene is identical to the human *Dkk (dickkopf)-3* gene (2), a member of the Dkk family of genes (*hDkk-1*, *hDkk-2*, *hDkk-3*, and *hDkk-4*), which encodes secreted regulatory factors of the Wnt/β-catenin signalling pathway and plays critical roles in many essential biological processes and a variety of diseases (3). *REIC* expression is epigenetically silenced in a variety of cancers (4), and *REIC* re-expression suppresses the proliferation of different types of cancer cells (3). Among these physiological functions, *REIC* has been recently described as a physiological endoplasmic reticulum (ER) stressor (5). Indeed, gene therapy using an adenovirus-carrying *REIC* increases ER stress chaperone BiP (GRP78) expression and thereafter induces JNK-mediated apoptotic cell death in different types of cancer cells (6) and does not cause non-cancer cell death but the production of interleukin (IL) 7 to reinforce the survival of natural killer cells (7). In addition, REIC protein is capable of inducing the differentiation of mononuclear leukocytes into dendritic cell (DC)–like cells (8), resulting in systemic augmentation of anti-tumour immune responses. These characteristics are fundamental properties of adenovirus-mediated *REIC* gene therapy. Based on these findings, phase I–IIa studies of Ad-REIC gene therapy in several cancer patients are ongoing (9, 10).

Immune checkpoint inhibitors, a type of immunotherapy, block immune checkpoint proteins from binding to co-inhibitory molecules (11). Anti-programmed death 1 (anti-PD-1) antibody and anti-cytotoxic-T-lymphocyte-associated protein 4 (CTLA-4) antibody therapy has demonstrated to have a durable response across different cancer types, and these initial clinical successes have unveiled a new area in cancer immunotherapy (12). However, durable clinical responses were only seen in 20-30% of cancer patients, implying that pre-existing anti-tumour immunity is crucial for the reactivity to immune checkpoint blockade (ICB) therapies (12). To date, several positive prognostic factors, such as the number of tumour-infiltrating lymphocytes (TILs), tumour PD-L1 expression, high tumour mutational burden, the existence of tumour neoantigens, and an interferon γ (*IFN-γ*) gene

Correspondence to: Kenji Araki, Watarase Research Center, Kyorin Pharmaceutical Co., Ltd., 1848, Nogi, Nogi-machi, Shimotsuga-gun, Tochigi 329-0114, Japan. Tel: +81 280571551, Fax: +81 280572336, e-mail: kenji.araki@mb.kyorin-pharm.co.jp

Key Words: REIC, immunogenic cell death, anti-cancer immunity, gene therapy, adenovirus vector, immune checkpoint inhibitors.

expression signature, have been identified (13). Tumours, which intrinsically lose the expression of antigen-presenting molecules or are deficient in T cells, are less likely to respond to immune checkpoint inhibitors (14). The tumour microenvironment comprises cancer cells, immune cells, fibroblasts, adipocytes, endothelial cells, mesenchymal cells, and extracellular matrix. Metabolic reprogramming of the tumour microenvironment is induced by tumour-derived exosomes (15), and metabolic competition between immune cells and tumour cells promotes local immune escape and immune exhaustion (16). Therefore, a novel therapeutic strategy is required to generate an immunogenic tumour microenvironment and expand the number of patients who could benefit from immune checkpoint inhibitor therapy. One strategy to induce this conversion involves the use of pharmaceutical interventions that elicit immunogenic cell death (ICD) within the tumour (17). However, a limited number of anti-cancer drugs, including anthracyclines (18), oxaliplatin (19), radiation therapy (20), photodynamic therapy (21), and oncolytic viruses (22), have been reported to cause ICD.

ICD is defined as a type of cancer cell death that occurs with the release of highly immunostimulatory damage-associated molecular patterns (DAMPs), such as the extracellular emission of high-mobility group box 1 (HMGB-1) (23), adenosine triphosphate (ATP) (24), and the translocation of calreticulin (CRT) (25). Induction of ICD in the tumour microenvironment leads to efficient antigen presentation by DCs, and dying tumour cells function as tumour-specific neoantigen vaccines. Consequently, tumour neoantigen-specific $CD8^+$ T cells are generated and moved out of the tumour-draining lymph nodes into the tumour microenvironment, resulting in effector functions. However, until now, only a limited number of anti-cancer modalities have been reported as ICD inducers. Furthermore, a particular drug has usage limitations due to the genetic background, tissue origin, and local tumour microenvironment; therefore, it is highly desirable to explore other anti-cancer therapies that can augment tumour immunogenicity and thereafter determine the advantage of immune checkpoint inhibitors.

In this study, we determined whether Ad-REIC–induced apoptotic cell death can trigger ICD by examining the emission of DAMPs *in vitro* and the vaccination effect *in vivo*. For confirmation testing, we compared the anti-tumour effects with and without the host immune system. Finally, we determined immunological changes in the tumour microenvironment by putative ICD inducers and the combined effects of ICB therapies.

Materials and Methods

Cell culture. Murine mesothelioma AB12 cells were kindly provided by Suzawa *et al*. (26) and cultured in high-glucose Dulbecco's modified Eagle's medium (Thermo Fisher Scientific, Waltham, MA, USA; #11965) supplemented with 10% foetal bovine serum (Thermo Fisher Scientific) and 1% penicillin and streptomycin (Thermo Fisher Scientific; #15070063) and maintained on a 100-mm plastic dish (BD Biosciences, Franklin Lakes, NJ, USA; #353003) at 37˚C in an atmosphere containing 5% CO_2. Murine mesothelioma AB1-HA (European Collection of Animal Cell Cultures, Porton Down, UK; #12070506) and AB22 (European Collection of Animal Cell Cultures; #10092307) were cultured in RPMI-1640 (Thermo Fisher Scientific, Gibco; #11875) supplemented with 10% foetal bovine serum (Biowest, Nuaillé, France) and 1% penicillin and streptomycin. In the case of AB1-HA cell culture, the aminoglycoside antibiotic G-418 (Sigma-Aldrich, St Louis, MO, USA; #4727878001) solution was added at a final concentration of 400 μg/ml to the RPMI-1640 complete medium.

Antibodies and reagents. *InVivo*Plus polyclonal Syrian hamster IgG (Bio X Cell, West Lebanon, NH, USA; clone: N/A; #BP0087), *InVivo*Plus anti-mouse CTLA-4 (CD152) (Bio X Cell; clone: 9H10; #BP0131), *InVivo*Plus rat IgG2a isotype control, anti-trinitrophenol (Bio X Cell; clone: 2A3; #BE0290), and *InVivo*Plus anti-mouse PD-1 (CD279) (Bio X Cell; clone: RMP1-14; #BP0146) were purchased and used. These antibodies were diluted with endotoxin-free Dulbecco's phosphate-buffered saline (Merck Millipore, Billerica, MA, USA; #TMS-012-A) for intraperitoneal (*i.p.*) administration. Rat anti-mouse CD16/CD32 mouse BD Fc block (BD Biosciences, San Jose, CA, USA; clone: 2.4G2; #553142), PE-Cy7 rat anti-mouse CD44 (BD Biosciences; clone: IM7; #560569), FITC-Rat Anti-Mouse CD62L (BD Biosciences; clone: MEL-14; #561917), APC-Cy7 rat anti-mouse CD8a (BD Biosciences; clone: 53-6.7; #561967), and PerCP-Cy5.5 Mouse Anti-Mouse CD45.2 (BD Biosciences; clone: 104; #552950) were purchased and used. When these antibodies were used for immunostaining, all were diluted 100-fold before use. Mitoxantrone (Sigma-Aldrich; #M6545) and cisplatin (Sigma-Aldrich; #479306) were purchased and used.

Adenovirus infection. The full-length complementary DNA of the human *REIC/DKK-3* gene was integrated into a cosmid vector pAxCAwt and transferred into an E1/E2-deleted replication-deficient adenovirus type 5 vector with the CAG (cytomegalovirus early enhancer/chicken β-actin) promoter using the cosmid cassettes and Ad DNA-terminal protein complex (COS/TPC) method (Takara Bio, Shiga, Japan) (27). The super gene expression (SGE) system was constructed by inserting the triple translational enhancer sequences of human telomerase reverse transcriptase, simian virus 40, and cytomegalovirus downstream of the BGH polyA sequence (28). An adenoviral vector carrying the *LacZ* gene with a CAG (Figure 1 and Figure 2) or SGE promoter (Figure 3 and Figure 4) was used as the control vector. These adenoviral vectors were generated using five replication-incompetent serotype adenoviruses. AB12 cells were plated at a concentration of 1.0×10^6 cells per well in 6-well plate culture plates 24 h before infection (Greiner; Bio-One GmbH, Frickenhausen, Germany). On the day of infection, the cells were counted, and AB12 cells were infected at a multiplicity of infection (MOI) of 0, 100, or 300. After adenovirus incubation at 37˚C for 1 h, the complete medium was added to each well and incubated thereafter for 24 or 48 h.

Quantification of cell death by annexin V and propidium iodide (PI) staining. Cell death was quantified using the Annexin V Apoptosis Detection Kit APC (Thermo Fisher Scientific; #88-

8007-72) according to the manufacturer's instructions. The cells were detached using 0.05% trypsin/ethylenediaminetetraacetic acid (EDTA) solution and prepared at concentrations from 1.0 to 5.0×10^6 cells/ml, 24 or 48 h after adenovirus infection. One aliquot (100 μl) of the cell suspension was washed once with annexin V binding buffer and stained with 5.0 μl of APC-annexin V and 2.5 μl of PI for 15 min at room temperature. Stained cells were filtered using a 5-ml round-bottom tube with a 35-μm pore-size cell strainer cap to remove cell aggregates, and the annexin V^+ PI^- cells were measured using BD FACSAria I (BD Biosciences).

Quantification of ER stress using quantitative polymerase chain reaction *(PCR)*. Quantification of ER stress (unfolded protein response) was performed using real-time quantitative PCR. Infected cells were harvested 24 h after infection, and total RNA was purified using the RNeasy Plus Mini Kit (Qiagen, Valencia, CA, USA; #74134) according to the manufacturer's protocol. The concentration of the obtained RNA was measured using a Nanodrop 1000 (Thermo Fisher Scientific), and 2,000 ng of RNA was used along with SuperScript VILO Master Mix (Thermo Fisher Scientific; #11754050). Purified RNA samples were mixed with SuperScript IV VILO Master Mix according to the manufacturer's instructions, and the mixture was incubated at 25˚C for 10 min, 50˚C for 10 min, and 85˚C for 5 min. Reverse transcripts were diluted (1:10) with Ambion Nuclease-Free Water (Thermo Fisher Scientific) and used as a template for real-time PCR. Real-time PCR was performed using the StepOne PCR (Applied Biosystems, Foster City, CA, USA) in a MicroAmp Fast Optical 96-Well Reaction Plate (Thermo Fisher Scientific; #4346907). The PCR reaction was performed in a total volume of 20 μl using TaqMan Gene Expression Assays (20×) (listed in Table I) and TaqMan Fast Advanced Master Mix (2×) (Applied Biosystems; #4444557). The reaction conditions for amplification of DNA were 50˚C for 2 min, 95˚C for 20 s, 40 cycles of 95˚C for 1 s, and 60˚C for 20 s. The quantification of gene expression was performed by the *dd*CT method (29) using StepOne Software version 2.2 (Applied Biosystems). *18S* CT was used as an endogenous control.

Quantification of extracellular ATP and HMGB-1 release. Conditioned medium derived from AB12 mesothelioma cells was harvested, centrifuged at 300×*g* for 5 min, and stored at −80˚C. Extracellular ATP levels in the supernatant were quantified using an ATP Bioluminescence Assay Kit HS II (Roche Diagnostics, Mannheim, Germany; #11699709001) according to the manufacturer's protocol. The supernatant extracellular HMGB-1 level was determined using the HMGB-1 ELISA Kit II (Shino-Test Corporation, Tokyo, Japan; #326078738) according to the manufacturer's protocol. Absorbance and luminescence were measured using a FlexStation III (Molecular Device, San Jose, CA, USA).

Determination of cell surface CRT exposure. Cell surface CRT exposure was determined by staining with an antibody without permeabilization. The infected cells were harvested and washed twice with cell-staining buffer (BioLegend, San Diego, CA, USA; #420201). Aliquots (100 μl) of the cell suspension were blocked with 2 μl of purified anti-mouse CD16/32 (BioLegend; #101302) at 4˚C for 10 min. Thereafter, 1.0 μl of anti-CRT antibody (Abcam, Cambridge, MA, USA; #ab2907) or 10 μl of rabbit IgG, polyclonal Isotype Control (ChIP Grade) (Abcam; #ab171870) was added and incubated for 30 min at 4˚C. Further, these cells were washed once with cell-staining buffer and stained with goat anti-rabbit IgG (H+L) cross-adsorbed secondary antibody, Alexa Fluor 647 (Thermo Fisher Scientific; #A-21244, 1,000-fold dilution) for 30 min at 4˚C. After washing once with cell staining buffer, aliquots (200 μl) of the cell suspension were stained with 5.0 μl DAPI (4¢,6-diamidino-2-phenylindole, dilactate) (BioLegend; #422801). Stained cells were filtered using a 5-ml round bottom tube with a 35-μm pore-size cell strainer cap to remove cell aggregates and analysed using BD FACSAria I. The median fluorescence intensity (MFI) was assessed for non-apoptotic–gated cells ($DAPI^-$). The MFI from each sample was calculated by subtracting the anti-isotype-antibody-stained MFI from the anti-CRT antibody-stained MFI.

Co-culture of dying tumour cells with bone marrow-derived DCs. Bone marrow cells were harvested from BALB/c mouse bone marrow and cultured in 20 ng/ml GM-CSF (Peprotech, Princeton, NJ, USA; #315-03) containing complete RPMI-1640 with 2-mercaptoethanol in a 100-mm Petri dish (BD Falcon; #351029) for 7 days to generate DCs, as previously described by Lutz *et al*. (30). Forty-eight hours after Ad-CAG-REIC infection (at an MOI of 100), infected AB12 mesothelioma cells, including both dying and living cells with or without condition medium, were harvested and co-cultured with DCs at 1.0×10^6 cells/well. Twenty-four hours after co-culture of DCs and AB12 mesothelial cells, cells were harvested and then washed with cell-staining buffer (BioLegend; #420201), blocked with FcR blocking (Miltenyi Biotec; #130-092-575) and then stained with PE anti-mouse CD11c (BioLegend; #117307, 100-fold dilution) and APC anti-mouse CD86 (BioLegend; #104713, 100-fold dilution). Stained cells were filtered using a 5-ml round bottom tube with a 35-μm pore-size cell strainer cap to remove cell aggregates and were analysed using BD FACSAria I (BD Biosciences). The mean fluorescence intensity of CD86 gated on $CD11c^+$ DCs was analysed.

Evaluation of ICD (in vivo vaccination assay). All animal protocols were in compliance and approved by the Animal Use Committees of Okayama University Medical School (approval no. OKU-2015173) or approved in agreement with the Guidelines of the Institutional Animal Care or Use Committee of Watarase Research Center of Kyorin Pharmaceutical (approval no. 17-117). Female BALB/cAJcl mice (6 weeks old), purchased from Japan Clea Inc. (Tokyo, Japan), were used when 7 weeks old after domestication in a novel environment. ICD *in vivo* by vaccination assays was performed as reported previously (31). Murine mesothelioma AB12 cells were treated *in vitro* with a presumptive inducer of ICD, 10 μM mitoxantrone (25), or a putative non-ICD inducer, 300 μM cisplatin (19), for 24 h or adenovirus infection at an MOI of 100 or 300 for 48 h. Cells were then washed and resuspended in phosphate-buffered saline (PBS), and 3.0×10^6 AB12 cells were finally injected subcutaneously into the left flank of mice as vaccination under isoflurane anaesthesia (3%-4% for induction and 1%-3% for maintenance). Mice were divided into PBS control (n=18), mitoxantrone (n=9), Ad-CAG-REIC at an MOI of 100 (n=15), Ad-CAG-REIC at an MOI of 300 (n=4), Ad-SGE-REIC at an MOI of 100 (n=9), and cisplatin (n=5). The experiment was conducted as four independent examinations. Seven days after the vaccination, mice were inoculated with intact 1.0×10^6 AB12 cells in the right flank as a challenge site under isoflurane anaesthesia. The tumour

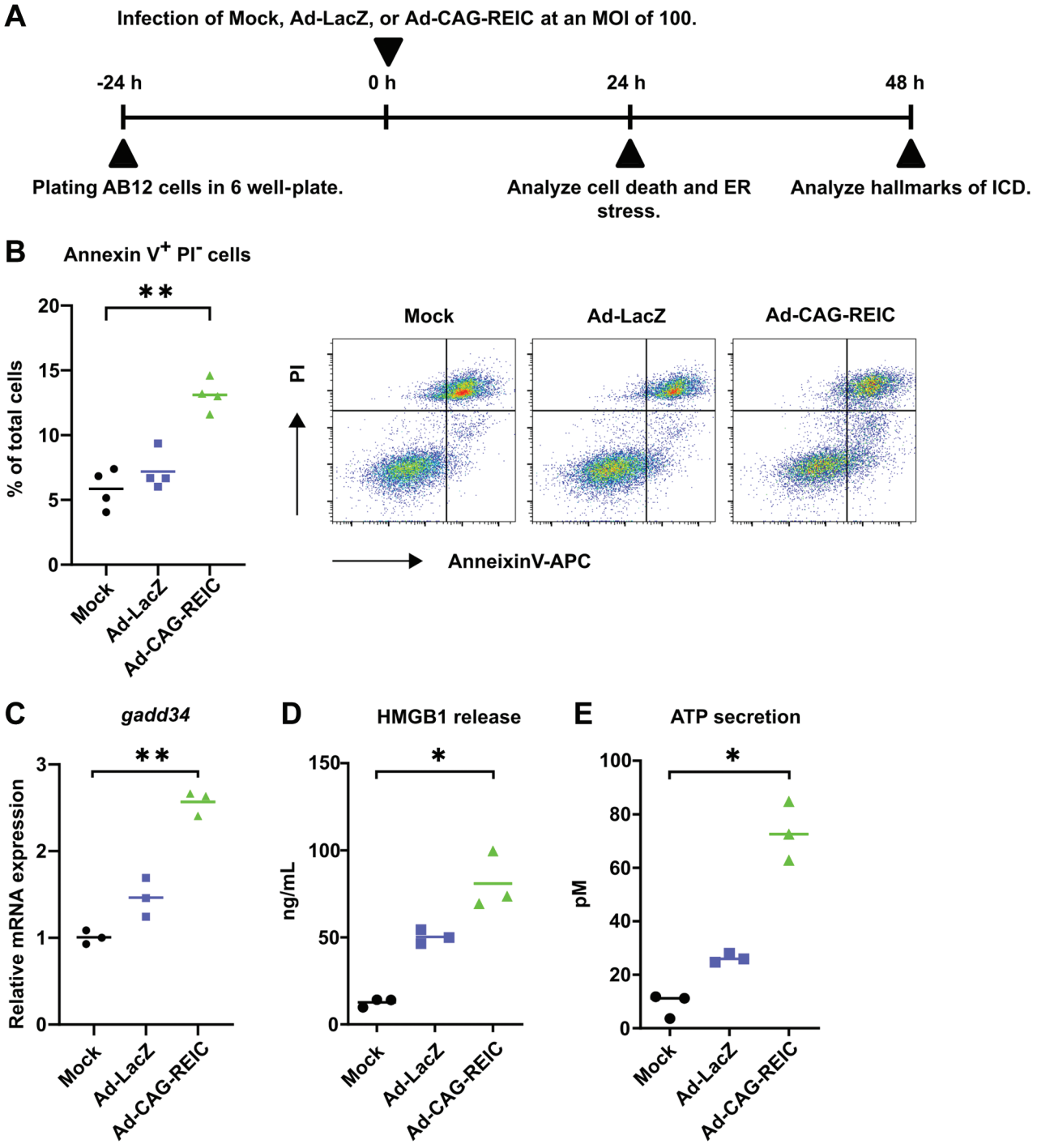

Figure 1. *Continued*

incidence rate was constantly observed at both vaccination and challenge sites over 41 days after AB12 challenge.

Evaluation of Ad-SGE-REIC on the immunocompetent mouse and immunodeficient mice models of mesothelioma AB12 and AB1-HA. As a confirmatory test for immunogenic cell death, specific pathogen-free immunodeficient BALB/cAJcl-*nu*/*nu* mice (aged 6 weeks) were purchased from Japan Clea Inc. and acclimatized for 1 week. When the tumours (AB12 and AB1-HA) reached a volume of 50-100 mm^3, the mice were divided into three groups, PBS treatment (n=5), Ad-LacZ (n=5), and Ad-SGE-REIC (n=5). Tumour volume was monitored at least twice a week by measurement using a digital

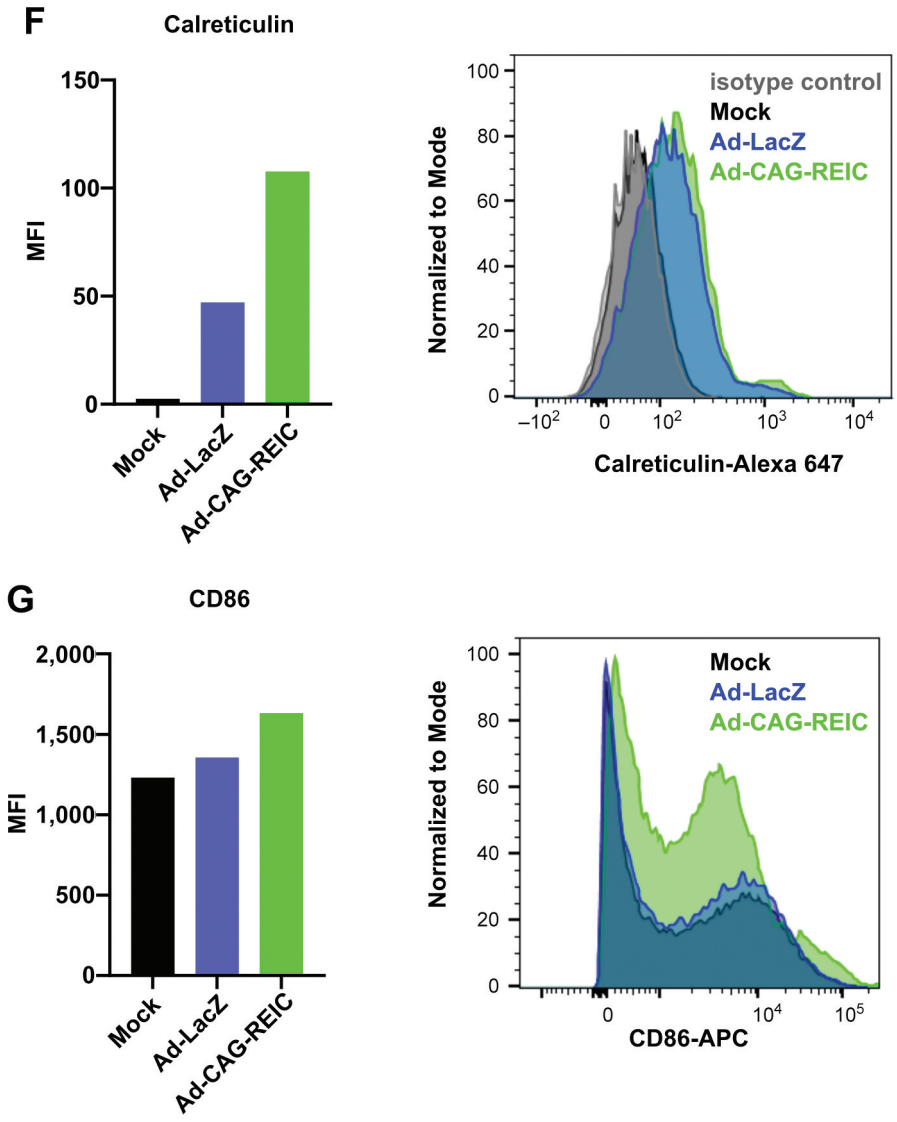

Figure 1. *Ad-CAG-REIC induces apoptotic cell death accompanied by the emission of ATP, HMGB-1, and the exposure of cellular surface CRT in murine mesothelioma AB12 cells. (A) The experimental protocol is shown. (B) Annexin V$^+$ and PI$^-$ cells % of total cells. Data presented are representative of the mean±standard error obtained from three independent experiments. A typical result is shown in a pseudo-color dot plot. (C) The mRNA expression level of gadd34. Investigations were performed in two independent experiments; the representative one is shown (dot plot shows technical replicates). (D) The concentration of HMGB-1. Data are presented as the mean±standard error of the mean obtained from three independent experiments, each performed in duplicate. (E) The concentration of ATP. Data are presented as the mean±standard error of the mean obtained from three independent experiments, each performed in duplicate. (F) Median fluorescence intensity and histogram of CRT. Investigations were performed in two independent experiments, and the representative one is shown. (G) Mean fluorescence intensity and histogram of CD86 with conditioned medium. Investigations were performed in two independent experiments, and the representative one is shown. *p<0.05, significantly different from mock-infected controls. ATP, Adenosine triphosphate; HMGBI-1, high mobility group box 1; CRT, calreticulin; mRNA, messenger RNA.*

calliper (Mitutoyo Corp, Tokyo, Japan) and approximated according to the formula $V=½\times a\times b^2$ (where *a* is the long diameter and *b* is the short diameter of the tumour). Tumour diameters were measured at least twice a week until 11 and 19 days after inoculation with AB12 and AB1-HA, respectively. The humane endpoint for euthanasia of mice was single tumour size greater than 2,000 mm^3 or total tumour (ipsilateral and contralateral) size greater than 3,000 mm^3.

Pathogen-free immunocompetent female BALB/cAJcl mice (aged 6 weeks) were purchased from Japan Clea Inc. and acclimatized for 1 week. One million cells of AB12 and AB1-HA cells were suspended in 100 μl of endotoxin-free PBS, and each cell line was inoculated intradermally into the bilateral flanks of mice (n=15 per each type of mesothelioma) under isoflurane anaesthesia. When the tumours reached a volume of 50-100 mm^3, the mice were

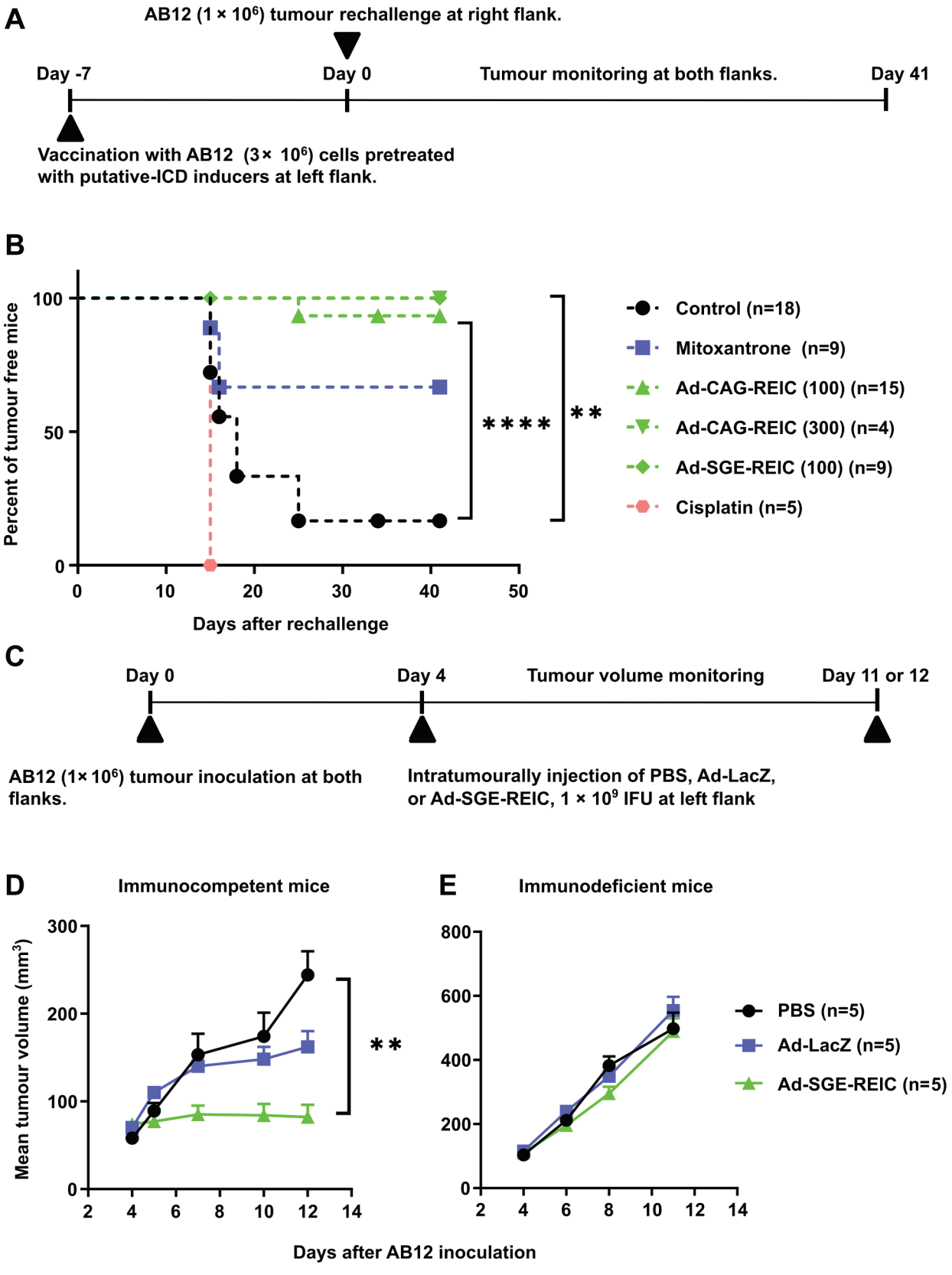

Figure 2. *Continued*

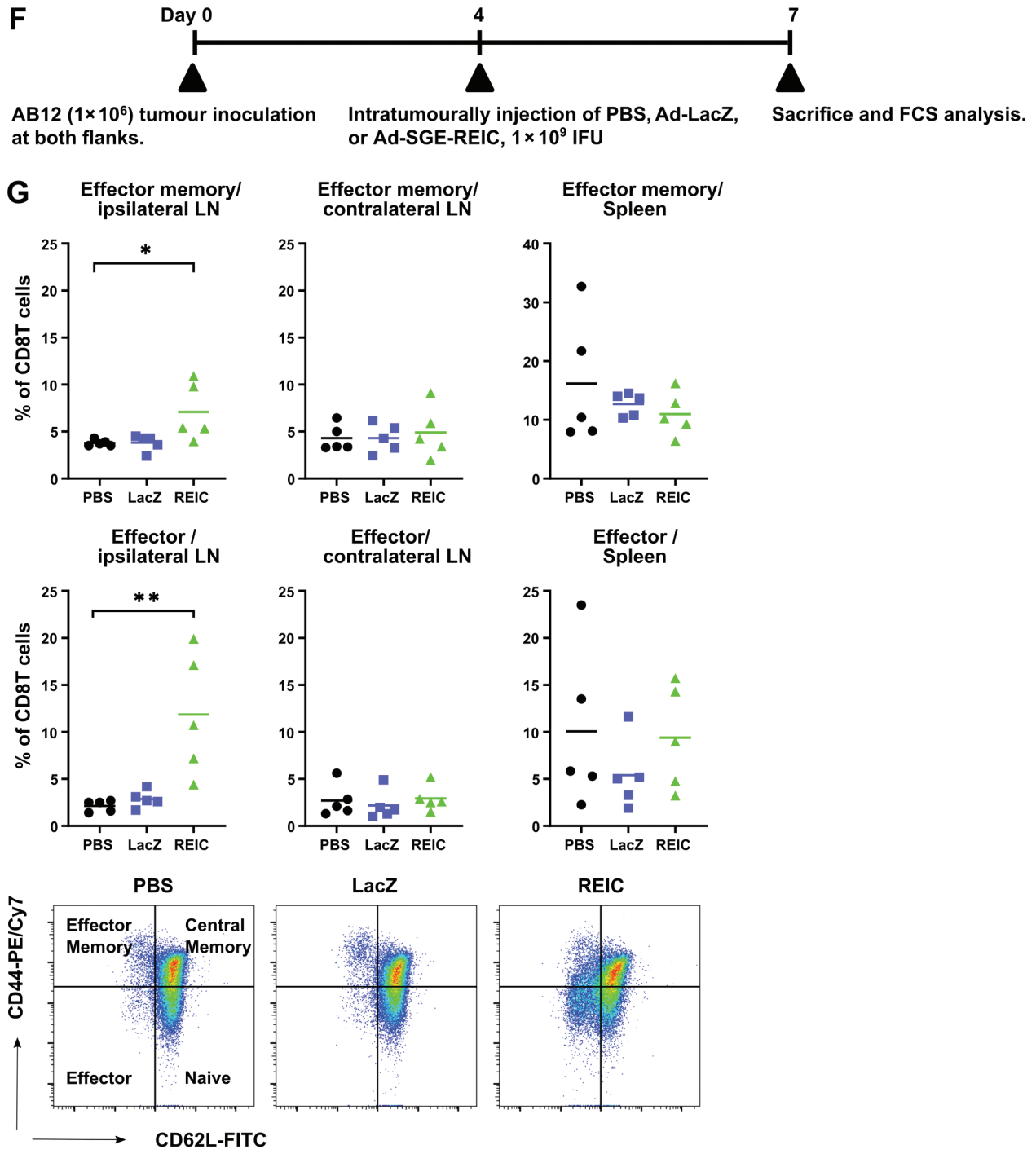

Figure 2. *Murine mesothelioma AB12 cells infected with Ad-CAG-REIC and Ad-SGE-REIC act as a therapeutic cancer vaccine. (A) The experimental protocol is shown. (B) The graph is showing the Kaplan–Meier curves indicating the percentage of tumour-free mice at the challenge site. The graph shows only events (palpable tumour growth). Log-rank tests were performed to compare treated cells to the control. (**p<0.01 and ****p<0.0001). (C) The experimental protocol is shown. Time-course changes of tumour volume was shown in immunocompetent mice (D) and immunodeficient mice (E) inoculated with AB12 cells receiving control (PBS), Ad-LacZ, or Ad-SGE-REIC intratumoural injection. The plot represents the mean±standard error of the mean of five animals. **p<0.01, significantly different from PBS-treated animals 11 days or 12 days after AB12 inoculation. (F) The experimental protocol is shown. (G) The X-axis shows treatment groups, and Y-axis indicates the population (%) of each CD8 T memory type. The analysis of a typical pseudo-color dot plot in the case of ipsilateral lymph nodes is shown. Individual plots show each animal. *p<0.05, **p<0.01, significantly different from PBS 7 days after AB12 inoculation. PBS, Phosphate-buffered saline; REIC, reduced expression in immortalized cell.*

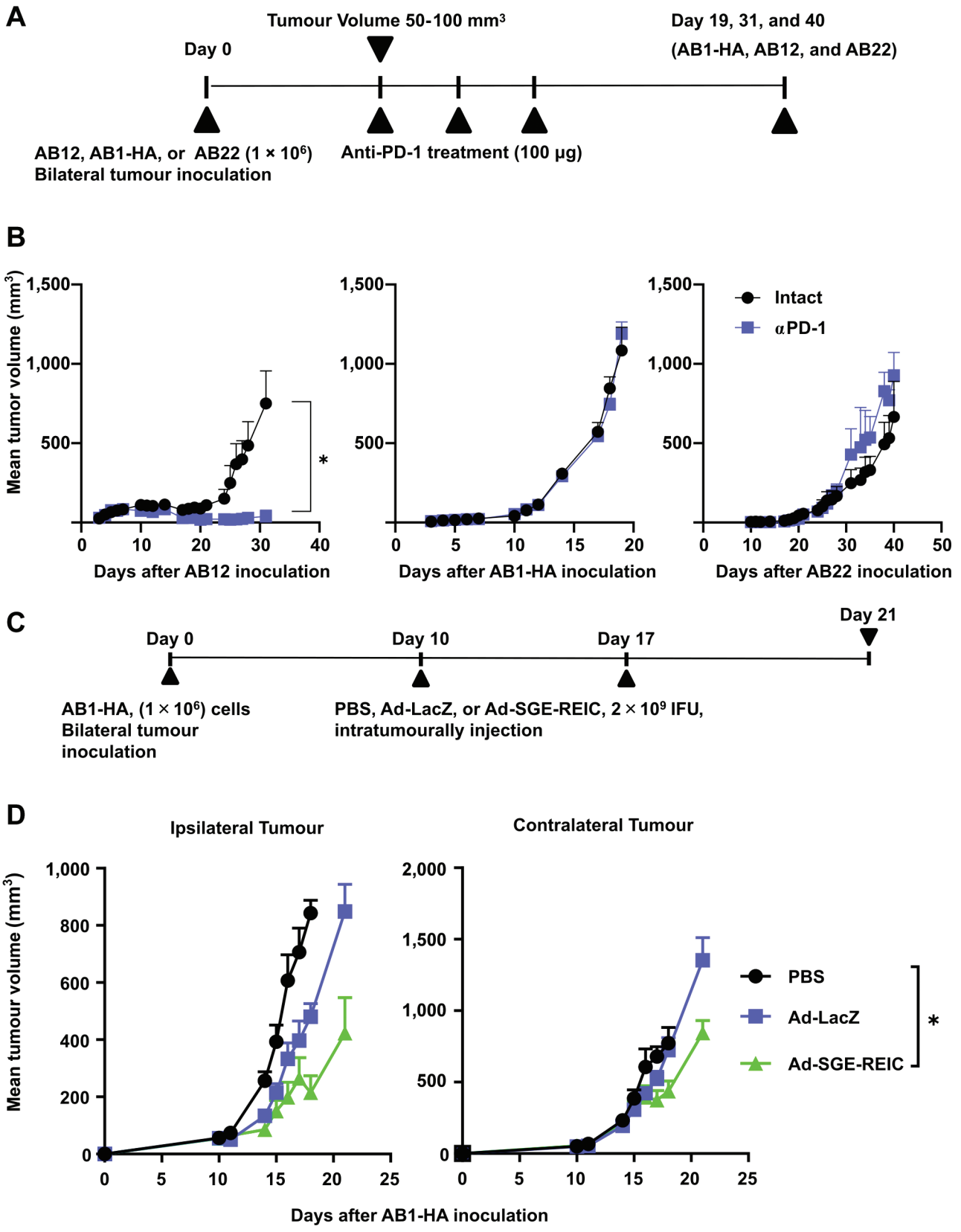

Figure 3. *Continued*

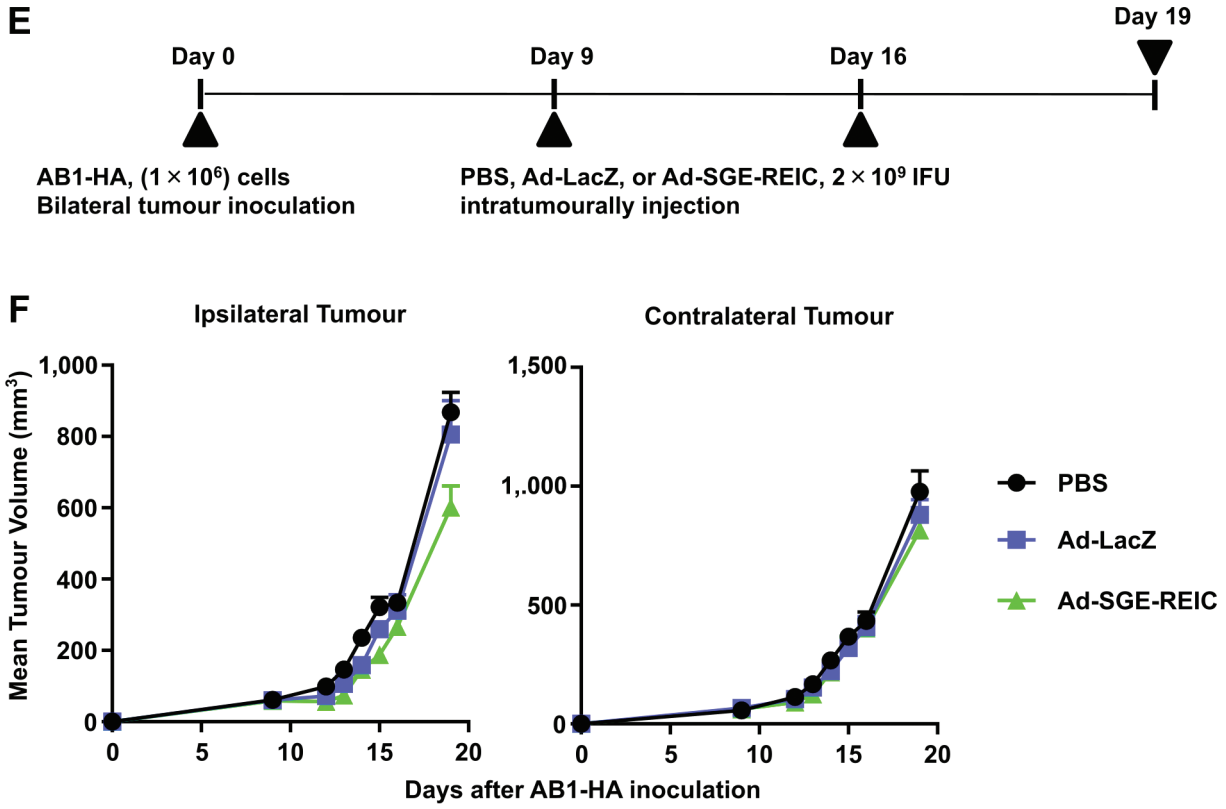

Figure 3. *Ad-SGE-REIC inhibits tumour growth in the syngeneic mouse model, which is refractory to anti-PD-1 antibodies. (A) The experimental protocol is shown. (B) Time-course changes of tumour volume (right side tumour volumes) in mice inoculated with AB1-HA cells receiving no (n=10) or anti-PD-1 (n=5). The plot represents the mean±standard error of the mean of 5-10 animals. *p<0.05, significantly different from non-treated animals 31 days after AB12 inoculation. (C) The experimental protocol is shown. (D) Time-course changes of tumour volume in immunocompetent mice inoculated with AB1-HA cells receiving control treatment PBS, Ad-LacZ, or Ad-SGE-REIC intratumoural injection. *p<0.05, **p<0.01, significantly different from PBS-treated animals 18 days after AB1-HA inoculation. (E) The experimental protocol is shown. (F) Time-course changes of tumour volume in immunodeficient mice inoculated with AB1-HA cells receiving control treatment PBS, Ad-LacZ, or Ad-SGE-REIC intratumoural injection. The plot represents the mean±standard error of the mean of five animals. anti-PD-1, Anti-programmed death 1; PBS, phosphate-buffered saline.*

divided into three groups according to the tumour volume, PBS-treatment (n=5), Ad-LacZ (n=5), and Ad-SGE-REIC (n=5) in the case of AB12 and AB1-HA. Tumour diameters were measured until 12 and 21 days after inoculation of tumours with AB12 and AB1-HA, respectively.

Evaluation of anti-PD-1 antibodies on syngeneic mouse models of mesothelioma (AB12, AB1-HA, and *AB22).* Pathogen-free immunocompetent female BALB/cAJcl mice (aged 6 weeks) were purchased and acclimatized for 1 week. One million cells were suspended in 100 μl of endotoxin-free PBS. Each cell line was inoculated intradermally into the bilateral flanks of mice (n=15 per type of mesothelioma). When the tumours reached a volume of 50-100 mm^3, the mice were divided into two groups, non-treatment (n=10) and anti-PD-1 treatment group (n=5), according to the tumour volume, and then anti-PD-1 antibody (100 mg) was administered by *i.p.* injection every 3 or 4 days for a total of three injections. Tumour diameters were measured at least twice a week. Tumour diameters were measured at least twice a week until 31, 19, and 40 days after tumour inoculation with AB12, AB1-HA, and AB22, respectively.

Evaluation of combinational therapy on syngeneic mouse models of mesothelioma (AB1-HA). Pathogen-free immunocompetent female BALB/cAJcl mice (aged 6 weeks) were purchased from Japan Clea Inc. and acclimatized for 1 week. When the tumours reached a volume of 50-100 mm^3, the mice were divided into four groups, isotype antibody control (n=5), anti-PD-1 treatment group (n=5), Ad-SGE-REIC (n=5), and Ad-SGE-REIC with anti-PD-1 treatment (n=5). Tumour diameters were measured until 24 days after tumour inoculation. To assess the effect of combination therapy with CTLA-4 inhibitors, the mice were divided into isotype antibody control (n=5), anti-CTLA-4 treatment group (n=5), Ad-SGE-REIC (n=5), and Ad-SGE-REIC with anti-CTLA-4 treatment (n=5). Tumour diameters were measured until 35 days after tumour inoculation.

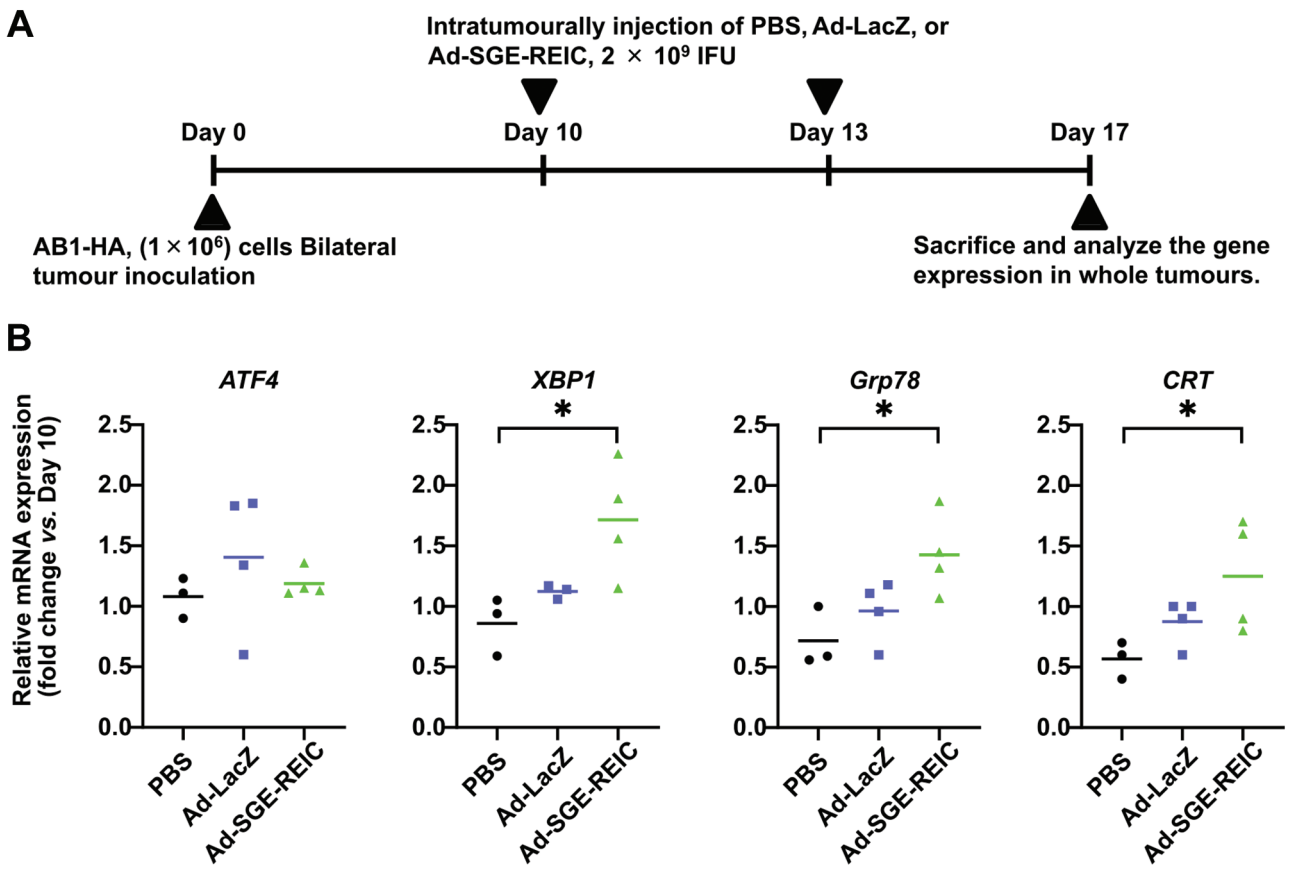

Figure 4. *Continued*

Analysis of CD8⁺ T-cell memory phenotypes in secondary lymphoid tissue. Pathogen-free immunocompetent female BALB/cAJcl mice aged 6 weeks were purchased from Japan Clea Inc. and used after 1 week of acclimatization. AB12 cells (1×10^6) were suspended in 100 μl of endotoxin-free PBS and inoculated intradermally into the bilateral flanks of mice (n=15) under isoflurane anaesthesia. When the tumours reached a volume of 50-100 mm^3, the mice were divided into groups according to the tumour volume and then administered by intratumoural injection of Ad-SGE-REIC (n=5), Ad-LacZ (n=5), or PBS (n=5) at a dose of 1.0×10^9 infection-forming units (IFUs) into the left flank tumour under isoflurane anaesthesia. At the indicated time, mice were euthanized by cervical dislocation, and both the spleen and lymph nodes were harvested, minced with a razor, and transferred into gentleMACS C Tube (Miltenyi Biotec) filled with FACS buffer (PBS containing 5 mM EDTA and 2% FBS) and homogenized with gentleMACS Octo Dissociator with Heaters using gentleMACS m_Spleen01 program. Cell suspensions were passed through a 70-μm nylon cell strainer (Falcon; #352350) and used for immunostaining. In the case of splenocytes, red blood cells were removed using ACK lysis buffer (Thermo Fisher Scientific, Gibco; #A1049201). Cells were washed twice with PBS, and dead cells were stained with LIVE/DEAD Fixable Aqua Dead Cell Stain Kit, for 405-nm excitation (Invitrogen; #L34957), according to the manufacturer's protocol. The cells were washed twice and suspended in 100 μL of FACS buffer. Cells were blocked with Purified Rat Anti-Mouse CD16/CD32 and stained with each antibody for 30 min on ice. Thereafter, the cells were washed with 2 ml of FACS buffer and fixed with 1% paraformaldehyde (Wako Pure Chemical Industries, BD; #553141) for 20 min at room temperature. Further, the cells were washed with 2 ml of FACS buffer and analysed using BD FACS Verse (BD Bioscience).

Analysis of gene expression profile of the tumour microenvironment. At the indicated time, AB1-HA-bearing mice were killed by cervical dislocation, and tumour tissues were harvested, minced using a razor, and immersed in RNAlater Stabilization Solution (Invitrogen; #AM7021) overnight at 4˚C, and subsequently stored at −80˚C. To isolate total RNA, frozen tissues were transferred into gentleMACS M Tube (Miltenyi Biotec) filled with Buffer RLT Plus, which was part of the RNeasy Plus Mini Kit and homogenized with gentleMACS Octo Dissociator with Heaters using gentleMACS Program RNA_02. Thereafter, total RNA was purified using the RNeasy Plus Mini Kit according to the manufacturer's protocol. After measuring the concentration of RNA by Nanodrop 2000 (Thermo Fisher Scientific), 2,000 ng of RNA was reverse transcribed using SuperScript VILO Master Mix SuperScript (Life Technologies, Foster City, CA; #11754050) following the manufacturer's instructions, and the mixture was incubated at 25˚C

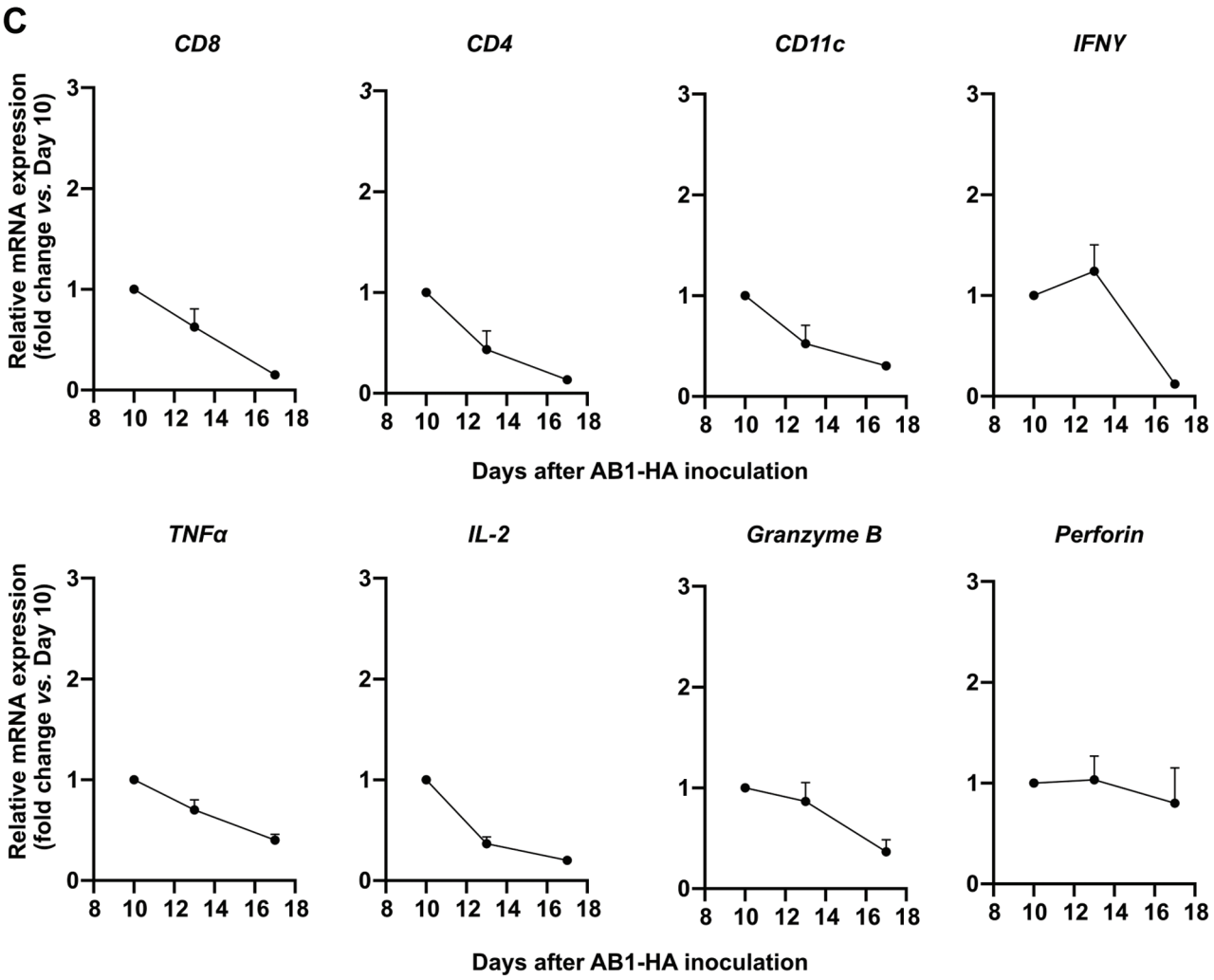

Figure 4. *Continued*

for 10 min, 50˚C for 10 min, and 85˚C for 5 min. Reverse transcripts were diluted (1:10) with Ambion Nuclease-Free Water (Thermo Fisher Scientific) and used as a template for real-time PCR. Real-time PCR was performed in combination with TaqMan Gene Expression Assays and TaqMan Fast Advanced Master Mix (Applied Biosystems; #4444557) on the ViiA 7 Real-time PCR System (Life Technologies). The TaqMan Gene Expression Assay IDs are listed in Table I.

Statistical analyses. Statistical analyses were performed using GraphPad Prism version 8.4.3 (GraphPad Software, Inc., San Diego, CA, USA). Data are expressed as the mean±standard error of the mean. A two-tailed unpaired Student's *t*-test was used to compare the differences between two groups, whereas one-way analysis of variance followed by Dunnett's post hoc test was used to compare the difference between multiple groups. In the case of vaccine experiments, log-rank tests were performed to compare treated cells to the control (PBS). For all comparisons, $p<0.05$ was considered statistically significant.

Results

Ad-CAG-REIC induces the emission of ATP and HMGB-1 and exposure of cellular surface CRT in murine mesothelioma AB12 cells. First, AB12 mesothelioma cells were selected as a validation model since Suzawa *et al*. (26) showed potent systemic anti-tumour immunity by intratumoural injection of Ad-SGE-REIC. We investigated whether apoptotic cell death induced by Ad-REIC shows the typical features of ICD, such as CRT surface exposure, HMGB-1, ATP release, and ER stress in AB12 mesothelioma cells (Figure 1A). We confirmed an increase in the population of annexin V^+ and PI^- cells compared with the mock-infected control 24 h after infection (Figure 1B). Furthermore, cell death induced by Ad-CAG-REIC infection was approximately equal to that of the control virus 48 h after infection (data not shown). To confirm that apoptotic

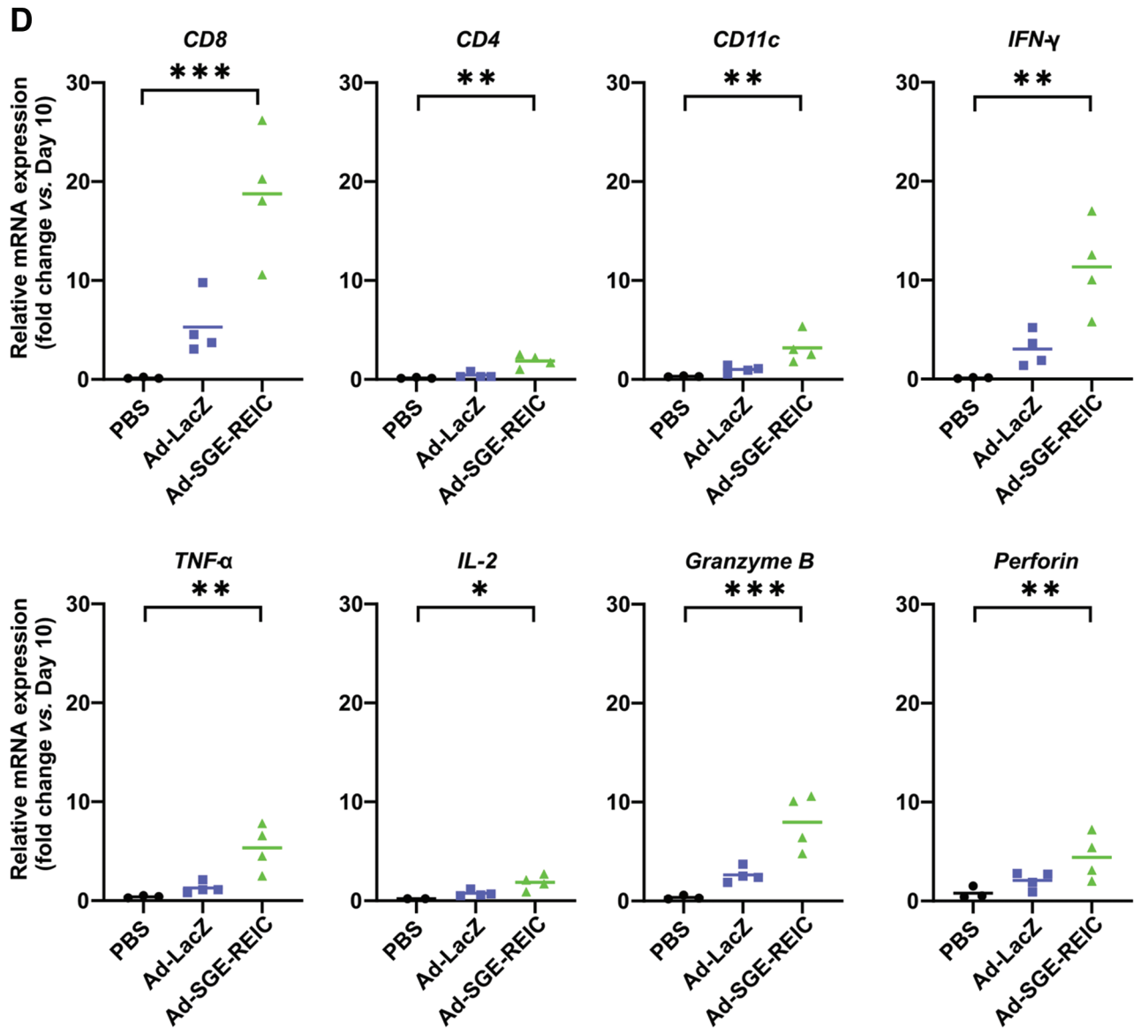

Figure 4. *Continued*

cell death was associated with ER stress, we analysed the induction of unfolded protein response (UPR) gene expression (*gadd34*, *XBP1*, *DNAjb9*, and *Grp78* were up-regulated by PERK, ATF6, IRE1, and the common UPR pathway, respectively). Among these genes, *gadd34* expression was selectively up-regulated by Ad-CAG-REIC infection (Figure 1C). Next, we investigated whether Ad-REIC treatment stimulates the extracellular release of HMGB-1 and ATP from AB12 mesothelial cells. As a result of the analysis, we observed an increase in HMGB-1 and ATP release into the conditioned medium 48 h after the infection compared with the mock-infected control (Figure 1D and E). Furthermore, we examined extracellular CRT exposure in living cells and found that CRT exposure increased 48 h after Ad-CAG-REIC infection (Figure 1F) compared to mock-infected cells. Finally, we examined whether these changes evoked activation of DCs. The mean fluorescence intensity of CD86 molecule expression on DCs increased 24 h after co-cultivation with AB12 mesothelioma cells infected with Ad-REIC (Figure 1G). Taken together, Ad-REIC induced DAMP release in AB12 cells, resulting in the activation of DCs.

AB12 infected with Ad-CAG-REIC or Ad-SGE-REIC acts as a therapeutic cancer vaccine. Next, we evaluated ICD *in vivo*. The experimental time course is shown in detail in

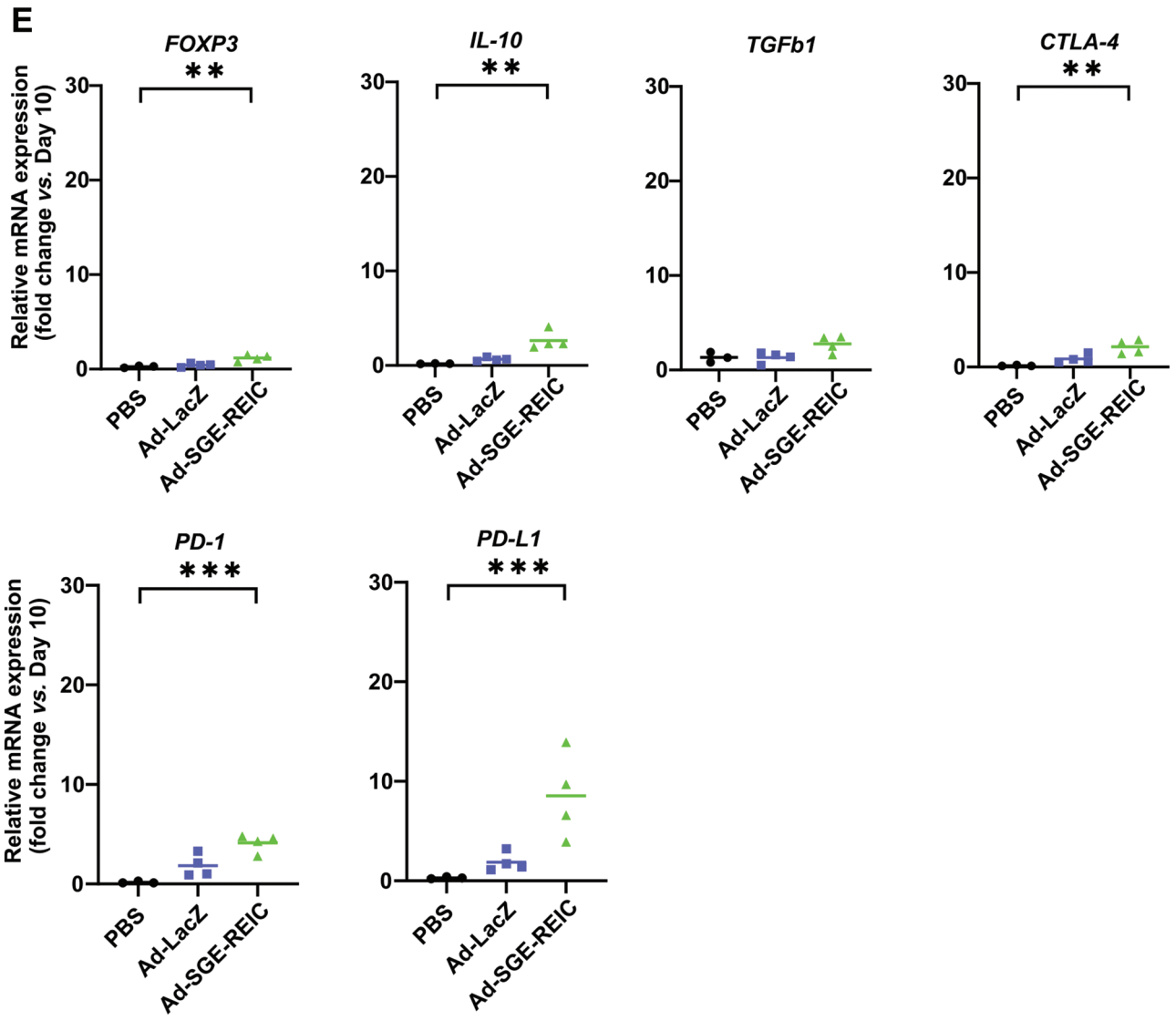

Figure 4. *Ad-SGE-REIC up-regulates the infiltration of CD8 T cells and up-regulates CD8 T cells effector molecules in the AB1-HA tumour microenvironment. (A) The experimental protocol is shown. (B) The Y-axis shows UPR-related gene expression (ATF4, XBP-1, Grp78, and CRT). (C) The X-axis shows days after PBS intratumoural injection, and the Y-axis shows anti-tumour immune response-related gene expression (CD8, CD4, CD11c, IFNg, TNFa, and IL-2). (D) The Y-axis shows anti-tumour immune response-related gene expression (CD8, CD4, CD11c, IFNg, TNFa, IL-2, GnzB, and perforin). (E) The Y-axis shows immunoregulatory gene expression (TGF-β, IL-10, FOXP3, PD-1, PD-L1, and CTLA-4). Individual plots show each animal. The plot represents the mean±standard error of the mean. *p<0.05, **p<0.01, ***p<0.001 significantly different from PBS-treated animals. PBS, Phosphate-buffered saline; UPR, unfolded protein response.*

Figure 2A. The results of the four independent experiments are summarized in Figure 2B. Seven days after vaccination, tumour formation was palpable at the vaccination site in the case of vaccination with non-treated AB12 and Ad-CAG-LacZ. In contrast, there was no tumour growth in the case of cisplatin, mitoxantrone, Ad-CAG-REIC, or Ad-SGE-REIC treatment at the vaccination site. Furthermore, mice inoculated with mitoxantrone, Ad-CAG-REIC, and Ad-SGE-REIC–infected AB12 cells showed no tumour growth at tumour challenge sites. Vaccination experiments showed that Ad-REIC infection induced ICD in AB12 cells *in vivo*. Next, we compared the anti-tumour effect in immunocompetent mice with immunodeficient tumour-bearing mice (Figure 2C, D, and E) by Ad-SGE-REIC for confirmation testing. The comparative analysis revealed that anti-tumour effects were noteworthy in immunocompetent mice models rather than in immunodeficient mice. Since antigens released by dying tumours are efficiently presented by DCs to naive or memory

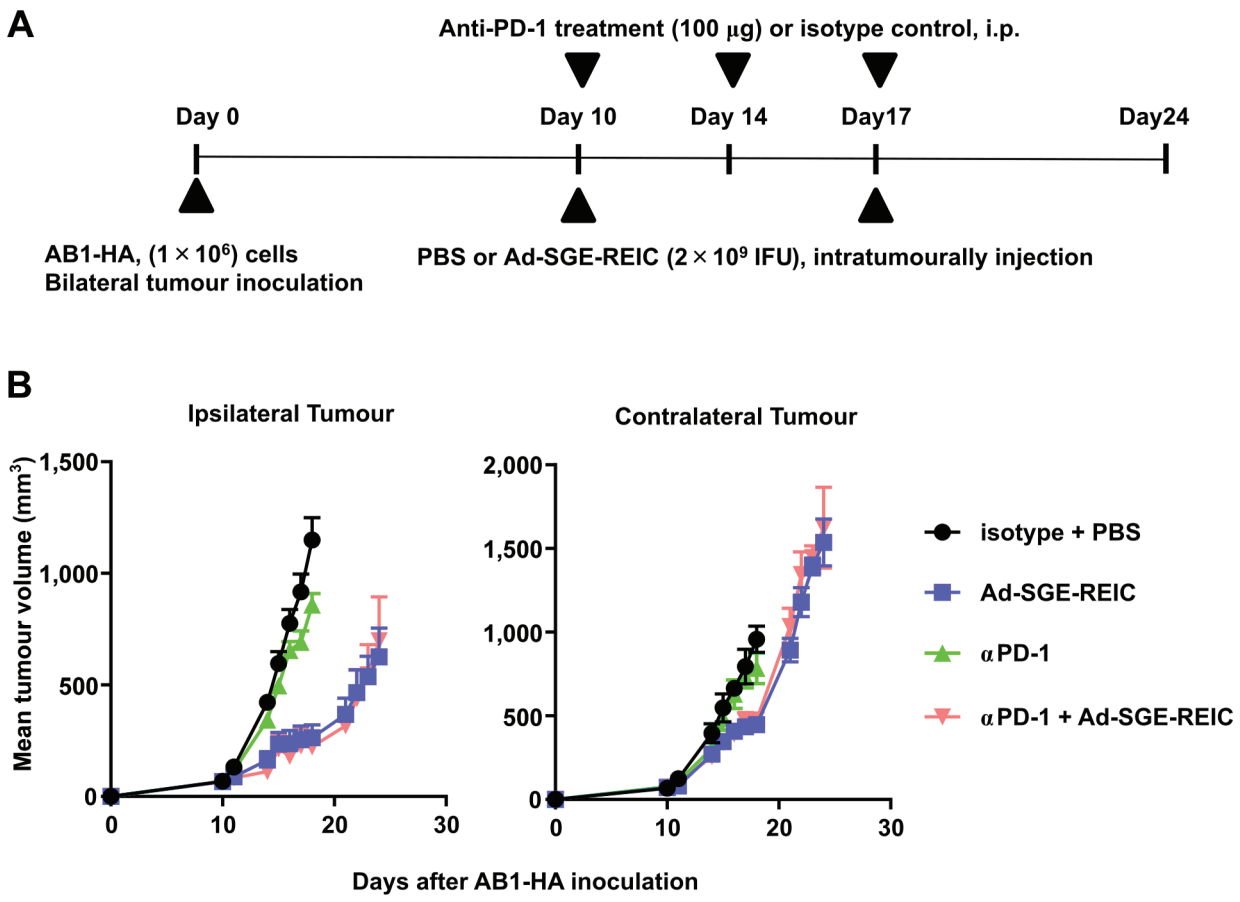

Figure 5. *Continued*

$CD8^+$T cells in the tumour-draining lymph nodes, we examined the change in $CD8^+$ T cells of the memory phenotype in secondary lymphoid tissues (Figure 2F and G). Consequently, the change in memory phenotype occurred, especially in the tumour-draining lymph nodes. In contrast, memory phenotype did not change in other secondary lymphoid tissues, such as the spleen and non-tumour draining lymph nodes. Based on these findings, we concluded that Ad-REIC acts as a *bona fide* inducer of ICD in murine mesothelioma AB12 cells.

Ad-SGE-REIC inhibits tumour growth in a murine mesothelioma AB1-HA cell model, which is refractory to anti-PD-1 antibodies. As described above, Ad-REIC induced ICD in AB12 mesothelial cells. Therefore, we expected that intratumoural Ad-REIC administration could change from a non-immunogenic tumour environment to an immunologically hot tumour microenvironment. To test this hypothesis, we first selected non-immunogenic murine mesothelioma cells by examining the effect of anti-PD-1 antibody therapy. Treatment with anti-PD-1 antibody completely inhibited AB12 cells at both flank sites, but not in the case of AB1-HA and AB22 mesothelioma cells (Figure 3A and B). Therefore, to determine immune reprogramming by Ad-REIC treatment, we selected murine mesothelioma AB1-HA and AB22 cells as immunologically cold tumour models. Ad-SGE-REIC showed modest growth inhibition of the tumour on the ipsilateral side and a slight inhibition on the contralateral side (Figure 3C and D). These anti-tumour effects were cancelled in the case of immunodeficient mice (Figure 3E and F). We did not observe any anti-tumour effect in the murine mesothelioma AB22 syngeneic mouse model because the murine mesothelioma AB22 cells had low *CXADR* expression and high *DKK3* expression, resulting in weak ER stress induction by Ad-REIC (data not shown).

Ad-SGE-REIC up-regulates the expression of CD8 and its effector molecules in the AB1-HA tumour microenvironment. Based on the results obtained from the study of the AB1-HA syngeneic mouse model, we expected that Ad-SGE-REIC would change the tumour microenvironment. To validate these changes, we analysed the gene expression profiles of the

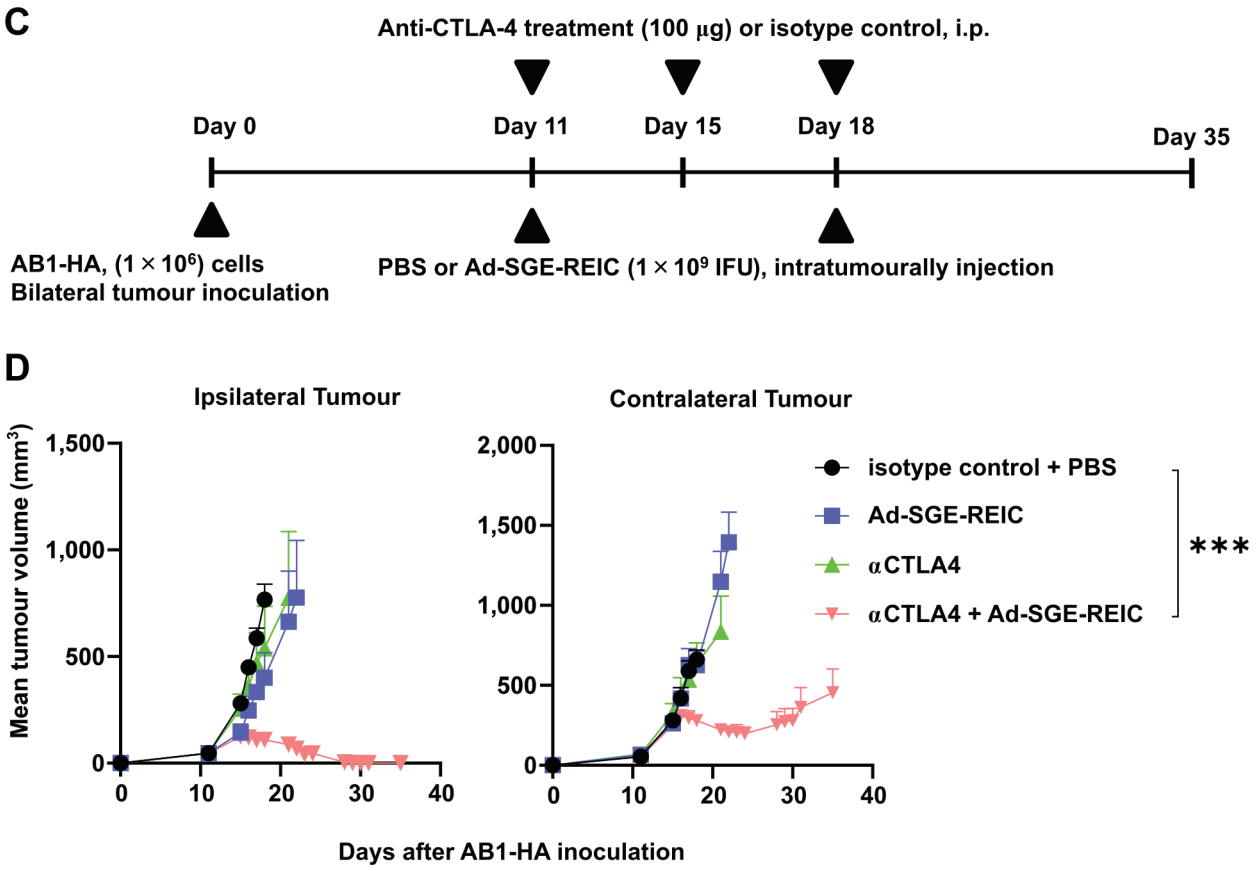

Figure 5. *Anti-CTLA-4 antibody therapy augments Ad-SGE-REIC-induced systemic immunity in AB1-HA syngeneic model. (A) The experimental design is shown. (B) Time-course changes of tumour volume in mice inoculated with AB1-HA cells receiving control treatment (i.p. injection of isotype control antibody with intratumoural injection of PBS), Ad-SGE-REIC monotherapy (i.p. injection of isotype control with intratumoural injection of Ad-SGE-REIC), anti-PD-1 monotherapy (i.p. injection of anti-PD-1 antibody with intratumoural injection of PBS), or combination therapy (i.p. injection of anti-PD-1 antibody with intratumoural injection of Ad-SGE-REIC). The plot represents the mean±SEM of five animals. (C) The experimental design is shown. (D) Time-course changes of tumour volume in mice inoculated with AB1-HA cells receiving control treatment (i.p. injection of isotype control antibody with intratumoural injection of PBS), Ad-SGE-REIC monotherapy (i.p. injection of isotype control antibody with intratumoural injection of Ad-SGE-REIC), anti-CTLA4 monotherapy (i.p. injection of anti-CTLA4 antibody with intratumoural injection of PBS), or combination therapy (i.p. injection of anti-CTLA4 antibody with intratumoural injection of Ad-SGE-REIC). The plot represents the mean±standard error of the mean of five animals. ***p<0.001, significantly different control treatment 18 days after AB1-HA inoculation. anti-PD-1, Anti-programmed death 1; CTLA-4, cytotoxic-T-lymphocyte-associated protein-4; i.p., intraperitoneal; PBS, phosphate-buffered saline.*

whole tumour injected with Ad-SGE-REIC in the AB1-HA model (Figure 4A). First, we confirmed the up-regulation of the gene expression levels of ER stress markers (*XBP1*, *Grp78*, and *CRT*) by Ad-SGE-REIC compared with the control (Figure 4B). In this model, the expression levels of anti-tumour immune response genes (*CD8*, *CD4*, *CD11c*, *IFNg*, *TNFa*, *IL-2*, *perforin*, *and granzyme B*) decreased at day 17 compared to those at day 10 after AB1-HA inoculation (Figure 4C). Next, we analysed the changes in immune-related gene expression in immunologically cold tumours after Ad-SGE-REIC treatment. We examined whether immune cells re-infiltrated the tumour tissue by ICD. We showed that Ad-REIC up-regulated the expression of *CD8* genes accompanied by increased lineage-specific gene expression (*CD4* and *CD11c*) and the expression levels of immune effector molecules (*IFN-γ*, *TNF-α*, *IL-2*, *perforin*, and *granzyme B*) (Figure 4D). In contrast, gene expression of immunoregulatory immune cells such as regulatory T cells (*FOXP3*), TGF-*b1*, and *IL-10* and the expression of T-cell exhaustion markers, including *PD-1*, *PD-L1*, and *CTLA-4*, were also increased (Figure 4E). These results showed that Ad-SGE-REIC induced the reprogramming of an immunologically cold tumour microenvironment.

Anti-CTLA-4 antibody therapy augments Ad-SGE-REIC-induced systemic immunity in the AB1-HA syngeneic model.

Table I. *Taqman gene expression assay used in this manuscript.*

Gene name	Taqman Assay ID
18s (18S ribosomal RNA)	Mm03928990_g1
Gadd34 (protein phosphatase 1, regulatory subunit 15A)	Mm01205601_g1
ATF4 (activating transcription factor 4)	Mm00515325_g1
Grp78 (heat shock protein 5)	Mm00517691_m1
XBP1 (X-box binding protein 1)	Mm00457357_m1
CRT (calreticulin)	Mm00482936_m1
CD4 (CD4 antigen)	Mm00442754_m1
CD8a (CD8 antigen, alpha chain)	Mm01182107_g1
Tgfb1(transforming growth factor, beta 1)	Mm01178820_m1
IL-10 (interleukin 10)	Mm00439614_m1
CD11c (integrin alpha X)	Mm00498701_m1
Gzmb (granzyme B)	Mm00442837_m1
Prf1 (perforin 1)	Mm00812512_m1
IFN-γ (interferon gamma)	Mm01168134_m1
IL-2 (interleukin 2)	Mm00434256_m1
Foxp3 (forkhead box P3)	Mm00475162_m1
PD-1 (programmed cell death 1)	Mm01285676_m1
PD-L1 (CD274 antigen)	Mm03048248_m1
CTLA-4 (cytotoxic T-lymphocyte associated protein 4)	Mm00486849_m1
TNF-α (tumor necrosis factor-α)	Mm00443258_m1

Because co-inhibitory molecules were increased by Ad-SGE-REIC, we tested whether two types of immune checkpoint inhibitors, anti-PD-1 and anti-CTLA-4, potentiate the Ad-SGE-REIC–mediated anti-tumour immune response. We first examined the effect of combination therapy with anti-PD-1 antibody and Ad-SGE-REIC treatment on AB1-HA cells at different dose combinations. In our experimental conditions, we did not observe any difference in the combination of anti-PD-1 treatment (100 μg/mouse) with Ad-SGE-REIC (2×10^9 IFU/mouse) (Figure 5A and B) compared with each monotherapy or at different dose combinations of anti-PD-1 treatment (200 μg/mouse) and Ad-SGE-REIC (1×10^9 IFU/mouse) (data not shown). Next, we examined the combined effect of anti-CTLA-4 treatment (100 μg/mouse) with Ad-SGE-REIC treatment (1×10^9 IFU/mouse). The combination therapy with anti-CTLA-4 treatment (100 μg/mouse) and Ad-SGE-REIC (1×10^9 IFU/mouse) completely blocked tumour growth in both flanks (Figure 5C and D). We also detected a synergistic effect in another dose combination of anti-CTLA-4 treatment (100 μg/mouse) and Ad-SGE-REIC treatment (2×10^9 IFU/mouse) (data not shown). Taken together, Ad-SGE-REIC–mediated anti-tumour immune response was enhanced by anti-CTLA-4 immunotherapy.

Discussion

Although Ad-REIC has a potential role in initiating ER stress (6), little is known about the involvement of Ad-REIC in ICD, especially with respect to the emission of DAMPs. In this study, we showed that Ad-REIC induces the release of HMGB-1 and ATP and the translocation of CRT in AB12 murine mesothelioma cells. We further showed that the vaccination effect is elicited by Ad-REIC treatment *in vivo*, which is a hallmark of ICD. Ad-REIC showed anti-tumour effects and the induction of ER stress markers and immunogenic reprogramming of the tumour microenvironment in murine mesothelioma AB1-HA cells, which are refractory to anti-PD-1 therapy. These changes were potentiated by anti-CTLA-4 antibody therapy. Altogether, these results showed that Ad-REIC acts as an ICD inducer *in vivo*, raising the possibility that combination therapy with anti-CTLA-4 antibody triggers a potent immune response in subjects with human mesothelioma.

Recently, ICD inducers have been classified into two groups [types I and II (32)]. Type I ICD inducers mainly comprise chemotherapeutic agents that evoke apoptotic cell death through non-ER-associated targets, such as DNA damage or proteasome inhibition, and up-regulate danger signalling *via* ER stress in an off-target manner. In contrast, type II inducers, such as photodynamic and oncolytic therapies, selectively target the ER to elicit CHOP or JNK-mediated apoptotic cell death and cause the release of danger signals in an ER-dependent manner. Ad-SGE-REIC is considered a type II ICD inducer because of its intensive ER stress–mediated apoptotic cell death. Type II ICD inducers, including photodynamic therapy and oncolytics, show anti-tumour immunity in a syngeneic mouse model (32). Anti-tumour immune responses induced by both photodynamic therapies (33) and oncolytic virus therapies (34) are potentiated by ICB therapies, including anti-PD-1, anti-PD-L1, and anti-CTLA-4 antibodies. Accordingly, we showed the combinational therapeutic effect of anti-CTLA-4 treatment and Ad-SGE-REIC, a putative ICD type II inhibitor. In our study, the improvement of immune exhaustion by anti-PD-1 treatment was definite, and anti-CTLA-4 antibody monotherapy caused more intensive anti-tumour immunity than anti-PD-1 treatment. These monotherapeutic effects were consistent with those reported by Fear *et al*. (35). Their study implied that terminally immune-exhausted $CD8^+$ T cells in the tumour microenvironment are non-responsive to anti-PD-1 therapy in murine mesothelioma AB1-HA cells. The authors showed the up-regulation of CTLA-4 molecules on regulatory T cells in the tumour-draining lymph nodes and the tumour microenvironment. Considering the strong monotherapeutic effect of CTLA-4 blockade, regulatory T-cell–mediated trans-endocytosis of B7 molecules of DCs (36) contributes largely to the immune escape of both local and systemic anti-tumour immunity. We inferred that the combination therapy of Ad-SGE-REIC and anti-CTLA-4 antibody enhances the efficient antigen presentation by DCs in the tumour-draining lymph node without being impaired by regulatory T-cell–mediated CTLA-4 dependent trans-endocytosis of B7 molecules.

These mechanisms can partially explain how Ad-REIC induces anti-tumour immune activation-related phenomena in

the bilateral tumour model, as we have previously reported (26, 37). In contrast, REIC protein itself has immune-modulatory functions *in vivo* (38), such as inducing monocytes into DC differentiation (8). In this study, we could not determine the contribution of REIC protein–mediated anti-tumour immune response to the anti-tumour immune effect by Ad-REIC because *REIC*-neutralizing antibodies are not available *in vivo*. The limitations of this study include the focus on malignant mesothelioma cells and the lack of investigation of other types of cancers, such as lung cancer (26) and lymphoma cells (37). Further studies are needed to reveal whether Ad-REIC can induce ICD as a general attribute regarding the emission of DAMPs and show the vaccination effect in other syngeneic mouse models. The exploration of the mechanism requires further investigation, including changes in TILs and maturation of DCs in the draining lymph node when combined with Ad-SGE-REIC and ICB therapy. In this study, changes in the tumour microenvironment were analysed by real-time PCR and only validated at the mRNA level. The lack of validation at the protein level and the lack of cell microscopy data are the major limitations of the present study. These experiments allowed us to analyse the subpopulation of immune cells infiltrating the tumour microenvironment and the interaction between immune cells and cancer cells. Knowing the spatial arrangement and co-localization of these cells will provide stronger support for our hypothesis.

The results obtained from these investigations support the hypothesis that Ad-REIC induces ICD in malignant mesothelioma. Ad-REIC acts as an ICD inducer *in vivo*, raising the possibility that combination therapy with anti-CTLA-4 antibody triggers a potent immune response in patients with mesothelioma.

Conflicts of Interest

KA and NY were employees of Kyorin Pharmaceutical Co., Ltd. Both authors conducted the study at their discretion and had editorial freedom with respect to the manuscript. The authors will not receive any monetary rewards from the company upon acceptance of the manuscript. Okayama University and Momotaro-Gene Inc. have patents for the SGE system, which was invented by HK. Momotaro-Gene Inc. holds the patents for the Ad-REIC and REIC protein agents and develops the agents as a cancer therapy medicine. HK owns stock in Momotaro-Gene Inc. Okayama University and Momotaro-Gene Inc. are working together to develop the Ad-REIC agent. Okayama University received research funds for joint research. HK is the chief scientific officer of Momotaro-Gene Inc.

Authors' Contributions

KA, NT, and HK conceived the study, KA and HK wrote the manuscript and generated the figures. KA, NT, and NY conducted the experiments. All Authors have read and approved the final manuscript.

Acknowledgements

We thank Dr. Junko Mori (Okayama University) for carefully reading and providing critical comments on this manuscript. This research was supported by the Newly Extended Technology Transfer Program (NexTEP) from the Japan Science and Technology Agency (JST) (grant number JPMJTT14N8).

References

1 Tsuji T, Miyazaki M, Sakaguchi M, Inoue Y and Namba M: A REIC gene shows down-regulation in human immortalized cells and human tumor-derived cell lines. Biochem Biophys Res Commun *268(1)*: 20-24, 2000. PMID: 10652205. DOI: 10.1006/bbrc.1999.2067

2 Krupnik VE, Sharp JD, Jiang C, Robison K, Chickering TW, Amaravadi L, Brown DE, Guyot D, Mays G, Leiby K, Chang B, Duong T, Goodearl AD, Gearing DP, Sokol SY and McCarthy SA: Functional and structural diversity of the human Dickkopf gene family. Gene *238(2)*: 301-313, 1999. PMID: 10570958. DOI: 10.1016/s0378-1119(99)00365-0

3 Veeck J and Dahl E: Targeting the Wnt pathway in cancer: the emerging role of Dickkopf-3. Biochim Biophys Acta *1825(1)*: 18-28, 2012. PMID: 21982838. DOI: 10.1016/j.bbcan.2011.09.003

4 Kobayashi K, Ouchida M, Tsuji T, Hanafusa H, Miyazaki M, Namba M, Shimizu N and Shimizu K: Reduced expression of the REIC/Dkk-3 gene by promoter-hypermethylation in human tumor cells. Gene *282(1-2)*: 151-158, 2002. PMID: 11814687. DOI: 10.1016/s0378-1119(01)00838-1

5 Fujita H, Bando T, Oyadomari S, Ochiai K, Watanabe M, Kumon H and Ohuchi H: Dkk3/REIC, an N-glycosylated protein, is a physiological endoplasmic reticulum stress inducer in the mouse adrenal gland. Acta Med Okayama *74(3)*: 199-208, 2020. PMID: 32577017. DOI: 10.18926/AMO/59950

6 Abarzua F, Sakaguchi M, Takaishi M, Nasu Y, Kurose K, Ebara S, Miyazaki M, Namba M, Kumon H and Huh NH: Adenovirus-mediated overexpression of REIC/Dkk-3 selectively induces apoptosis in human prostate cancer cells through activation of c-Jun-NH2-kinase. Cancer Res *65(21)*: 9617-9622, 2005. PMID: 16266978. DOI: 10.1158/0008-5472.CAN-05-0829

7 Sakaguchi M, Kataoka K, Abarzua F, Tanimoto R, Watanabe M, Murata H, Than SS, Kurose K, Kashiwakura Y, Ochiai K, Nasu Y, Kumon H and Huh NH: Overexpression of REIC/Dkk-3 in normal fibroblasts suppresses tumor growth *via* induction of interleukin-7. J Biol Chem *284(21)*: 14236-14244, 2009. PMID: 19279003. DOI: 10.1074/jbc.M808002200

8 Watanabe M, Kashiwakura Y, Huang P, Ochiai K, Futami J, Li SA, Takaoka M, Nasu Y, Sakaguchi M, Huh NH and Kumon H: Immunological aspects of REIC/Dkk-3 in monocyte differentiation and tumor regression. Int J Oncol *34(3)*: 657-663, 2009. PMID: 19212670. DOI: 10.3892/ijo_00000191

9 Oyama A, Shiraha H, Uchida D, Iwamuro M, Kato H, Takaki A, Ikeda F, Onishi H, Yasunaka T, Takeuchi Y, Wada N, Iwasaki Y, Sakata M, Okada H and Kumon H: A Phase I/Ib trial of Ad-REIC in liver cancer: study protocol. Future Oncol *15(31)*: 3547-3554, 2019. PMID: 31663777. DOI: 10.2217/fon-2019-0115

10 Kurozumi K, Fujii K, Shimazu Y, Tomita Y, Sasaki T, Yasuhara T, Hishikawa T, Kameda M, Kumon H and Date I: Study

protocol of a Phase I/IIa clinical trial of Ad-SGE-REIC for treatment of recurrent malignant glioma. Future Oncol *16(6)*: 151-159, 2020. PMID: 31973596. DOI: 10.2217/fon-2019-0743

11 Pardoll DM: The blockade of immune checkpoints in cancer immunotherapy. Nat Rev Cancer *12(4)*: 252-264, 2012. PMID: 22437870. DOI: 10.1038/nrc3239

12 Gong J, Chehrazi-Raffle A, Reddi S and Salgia R: Development of PD-1 and PD-L1 inhibitors as a form of cancer immunotherapy: a comprehensive review of registration trials and future considerations. J Immunother Cancer *6(1)*: 8, 2018. PMID: 29357948. DOI: 10.1186/s40425-018-0316-z

13 Maleki Vareki S, Garrigós C and Duran I: Biomarkers of response to PD-1/PD-L1 inhibition. Crit Rev Oncol Hematol *116*: 116-124, 2017. PMID: 28693793. DOI: 10.1016/j.critrevonc.2017.06.001

14 Trujillo JA, Sweis RF, Bao R and Luke JJ: T Cell-inflamed *versus* non-T cell-inflamed tumors: A conceptual framework for cancer immunotherapy drug development and combination therapy selection. Cancer Immunol Res *6(9)*: 990-1000, 2018. PMID: 30181337. DOI: 10.1158/2326-6066.CIR-18-0277

15 Yang E, Wang X, Gong Z, Yu M, Wu H and Zhang D: Exosome-mediated metabolic reprogramming: the emerging role in tumor microenvironment remodeling and its influence on cancer progression. Signal Transduct Target Ther *5(1)*: 242, 2020. PMID: 33077737. DOI: 10.1038/s41392-020-00359-5

16 Chang CH, Qiu J, O'Sullivan D, Buck MD, Noguchi T, Curtis JD, Chen Q, Gindin M, Gubin MM, van der Windt GJ, Tonc E, Schreiber RD, Pearce EJ and Pearce EL: Metabolic competition in the tumor microenvironment is a driver of cancer progression. Cell *162(6)*: 1229-1241, 2015. PMID: 26321679. DOI: 10.1016/j.cell.2015.08.016

17 Kepp O, Zitvogel L and Kroemer G: Clinical evidence that immunogenic cell death sensitizes to PD-1/PD-L1 blockade. Oncoimmunology *8(10)*: e1637188, 2019. PMID: 31646079. DOI: 10.1080/2162402X.2019.1637188

18 Fucikova J, Kralikova P, Fialova A, Brtnicky T, Rob L, Bartunkova J and Spísek R: Human tumor cells killed by anthracyclines induce a tumor-specific immune response. Cancer Res *71(14)*: 4821-4833, 2011. PMID: 21602432. DOI: 10.1158/0008-5472.CAN-11-0950

19 Tesniere A, Schlemmer F, Boige V, Kepp O, Martins I, Ghiringhelli F, Aymeric L, Michaud M, Apetoh L, Barault L, Mendiboure J, Pignon JP, Jooste V, van Endert P, Ducreux M, Zitvogel L, Piard F and Kroemer G: Immunogenic death of colon cancer cells treated with oxaliplatin. Oncogene *29(4)*: 482-491, 2010. PMID: 19881547. DOI: 10.1038/onc.2009.356

20 Golden EB and Apetoh L: Radiotherapy and immunogenic cell death. Semin Radiat Oncol *25(1)*: 11-17, 2015. PMID: 25481261. DOI: 10.1016/j.semradonc.2014.07.005

21 Korbelik M, Stott B and Sun J: Photodynamic therapy-generated vaccines: relevance of tumour cell death expression. Br J Cancer *97(10)*: 1381-1387, 2007. PMID: 17971767. DOI: 10.1038/sj.bjc.6604059

22 Liikanen I, Ahtiainen L, Hirvinen ML, Bramante S, Cerullo V, Nokisalmi P, Hemminki O, Diaconu I, Pesonen S, Koski A, Kangasniemi L, Pesonen SK, Oksanen M, Laasonen L, Partanen K, Joensuu T, Zhao F, Kanerva A and Hemminki A: Oncolytic adenovirus with temozolomide induces autophagy and antitumor immune responses in cancer patients. Mol Ther *21(6)*: 1212-1223, 2013. PMID: 23546299. DOI: 10.1038/mt.2013.51

23 Yamazaki T, Hannani D, Poirier-Colame V, Ladoire S, Locher C, Sistigu A, Prada N, Adjemian S, Catani JP, Freudenberg M, Galanos C, André F, Kroemer G and Zitvogel L: Defective immunogenic cell death of HMGB1-deficient tumors: compensatory therapy with TLR4 agonists. Cell Death Differ *21(1)*: 69-78, 2014. PMID: 23811849. DOI: 10.1038/cdd.2013.72

24 Martins I, Wang Y, Michaud M, Ma Y, Sukkurwala AQ, Shen S, Kepp O, Métivier D, Galluzzi L, Perfettini JL, Zitvogel L and Kroemer G: Molecular mechanisms of ATP secretion during immunogenic cell death. Cell Death Differ *21(1)*: 79-91, 2014. PMID: 23852373. DOI: 10.1038/cdd.2013.75

25 Obeid M, Tesniere A, Ghiringhelli F, Fimia GM, Apetoh L, Perfettini JL, Castedo M, Mignot G, Panaretakis T, Casares N, Métivier D, Larochette N, van Endert P, Ciccosanti F, Piacentini M, Zitvogel L and Kroemer G: Calreticulin exposure dictates the immunogenicity of cancer cell death. Nat Med *13(1)*: 54-61, 2007. PMID: 17187072. DOI: 10.1038/nm1523

26 Suzawa K, Shien K, Peng H, Sakaguchi M, Watanabe M, Hashida S, Maki Y, Yamamoto H, Tomida S, Soh J, Asano H, Tsukuda K, Nasu Y, Kumon H, Miyoshi S and Toyooka S: Distant bystander effect of REIC/DKK3 gene therapy through immune system stimulation in thoracic malignancies. Anticancer Res *37(1)*: 301-307, 2017. PMID: 28011506. DOI: 10.21873/anticanres.11321

27 Tani K, Lin T, Hibino H, Takahashi K, Nakazaki Y, Takahashi S, Nagayama H, Ozawa K, Saitoh I and Mulligan R: Transduction of LacZ gene into leukemia cells using viral vectors of retrovirus and adenovirus. Leukemia *9 Suppl 1*: S64-S65, 1995. PMID: 7475316.

28 Watanabe M, Sakaguchi M, Kinoshita R, Kaku H, Ariyoshi Y, Ueki H, Tanimoto R, Ebara S, Ochiai K, Futami J, Li SA, Huang P, Nasu Y, Huh NH and Kumon H: A novel gene expression system strongly enhances the anticancer effects of a REIC/Dkk-3-encoding adenoviral vector. Oncol Rep *31(3)*: 1089-1095, 2014. PMID: 24398705. DOI: 10.3892/or.2013.2958

29 Livak KJ and Schmittgen TD: Analysis of relative gene expression data using real-time quantitative PCR and the 2(-Delta Delta C(T)) Method. Methods *25(4)*: 402-408, 2001. PMID: 11846609. DOI: 10.1006/meth.2001.1262

30 Lutz MB, Kukutsch N, Ogilvie AL, Rössner S, Koch F, Romani N and Schuler G: An advanced culture method for generating large quantities of highly pure dendritic cells from mouse bone marrow. J Immunol Methods *223(1)*: 77-92, 1999. PMID: 10037236. DOI: 10.1016/s0022-1759(98)00204-x

31 Kepp O, Senovilla L, Vitale I, Vacchelli E, Adjemian S, Agostinis P, Apetoh L, Aranda F, Barnaba V, Bloy N, Bracci L, Breckpot K, Brough D, Buqué A, Castro MG, Cirone M, Colombo MI, Cremer I, Demaria S, Dini L, Eliopoulos AG, Faggioni A, Formenti SC, Fučíková J, Gabriele L, Gaipl US, Galon J, Garg A, Ghiringhelli F, Giese NA, Guo ZS, Hemminki A, Herrmann M, Hodge JW, Holdenrieder S, Honeychurch J, Hu HM, Huang X, Illidge TM, Kono K, Korbelik M, Krysko DV, Loi S, Lowenstein PR, Lugli E, Ma Y, Madeo F, Manfredi AA, Martins I, Mavilio D, Menger L, Merendino N, Michaud M, Mignot G, Mossman KL, Multhoff G, Oehler R, Palombo F, Panaretakis T, Pol J, Proietti E, Ricci JE, Riganti C, Rovere-Querini P, Rubartelli A, Sistigu A, Smyth MJ, Sonnemann J, Spisek R, Stagg J, Sukkurwala AQ, Tartour E, Thorburn A, Thorne SH, Vandenabeele P, Velotti F, Workenhe ST, Yang H,

Zong WX, Zitvogel L, Kroemer G and Galluzzi L: Consensus guidelines for the detection of immunogenic cell death. Oncoimmunology *3(9)*: e955691, 2014. PMID: 25941621. DOI: 10.4161/21624011.2014.955691

32 Asadzadeh Z, Safarzadeh E, Safaei S, Baradaran A, Mohammadi A, Hajiasgharzadeh K, Derakhshani A, Argentiero A, Silvestris N and Baradaran B: Current approaches for combination therapy of cancer: the role of immunogenic cell death. Cancers (Basel) *12(4)*: 1047, 2020. PMID: 32340275. DOI: 10.3390/cancers12041047

33 Nath S, Obaid G and Hasan T: The course of immune stimulation by photodynamic therapy: Bridging fundamentals of photochemically induced immunogenic cell death to the enrichment of T-cell repertoire. Photochem Photobiol *95(6)*: 1288-1305, 2019. PMID: 31602649. DOI: 10.1111/php.13173

34 Sivanandam V, LaRocca CJ, Chen NG, Fong Y and Warner SG: Oncolytic viruses and immune checkpoint inhibition: The best of both worlds. Mol Ther Oncolytics *13*: 93-106, 2019. PMID: 31080879. DOI: 10.1016/j.omto.2019.04.003

35 Fear VS, Tilsed C, Chee J, Forbes CA, Casey T, Solin JN, Lansley SM, Lesterhuis WJ, Dick IM, Nowak AK, Robinson BW, Lake RA and Fisher SA: Combination immune checkpoint blockade as an effective therapy for mesothelioma. Oncoimmunology *7(10)*: e1494111, 2018. PMID: 30288361. DOI: 10.1080/2162402X.2018.1494111

36 Ovcinnikovs V, Ross EM, Petersone L, Edner NM, Heuts F, Ntavli E, Kogimtzis A, Kennedy A, Wang CJ, Bennett CL, Sansom DM and Walker LSK: CTLA-4-mediated transendocytosis of costimulatory molecules primarily targets migratory dendritic cells. Sci Immunol *4(35)*: eaaw0902, 2019. PMID: 31152091. DOI: 10.1126/sciimmunol.aaw0902

37 Ariyoshi Y, Watanabe M, Eikawa S, Yamazaki C, Sadahira T, Hirata T, Araki M, Ebara S, Nasu Y, Udono H and Kumon H: The induction of antigen-specific CTL by *in situ* Ad-REIC gene therapy. Gene Ther *23(5)*: 408-414, 2016. PMID: 26836118. DOI: 10.1038/gt.2016.7

38 Kinoshita R, Watanabe M, Huang P, Li SA, Sakaguchi M, Kumon H and Futami J: The cysteine-rich core domain of REIC/Dkk-3 is critical for its effect on monocyte differentiation and tumor regression. Oncol Rep *33(6)*: 2908-2914, 2015. PMID: 25823913. DOI: 10.3892/or.2015.3885

Received August 5, 2021
Revised August 30, 2021
Accepted September 2, 2021